

Phased Array Antenna Pattern Variation with Frequency and Implications for Radar Spectrum Measurements

Frank H. Sanders
Bradley J. Ramsey



report series

Phased Array Antenna Pattern Variation with Frequency and Implications for Radar Spectrum Measurements

**Frank H. Sanders
Bradley J. Ramsey**



**U.S. DEPARTMENT OF COMMERCE
Carlos M. Gutierrez, Secretary**

Michael D. Gallagher, Assistant Secretary
for Communications and Information

December 2005

ACKNOWLEDGEMENT

The work presented in this report was performed under a cooperative research and development agreement (CRADA) between NTIA and the RF Metrics Corporation. The NTIA/ITS field site at Table Mountain, north of Boulder, Colorado, was used to perform the measurements presented in this report.

DISCLAIMER

Certain commercial equipment and materials are identified in this report to specify adequately the technical aspects of the reported results. In no case does such identification imply recommendations or endorsement by the National Telecommunications and Information Administration, nor does it imply that the material or equipment identified is the best available for this purpose.

CONTENTS

	Page
FIGURES	vi
TABLES	vi
ACRONYMS/ABBREVIATIONS.....	vi
1 INTRODUCTION	1
2 APPROACH.....	3
3 RESULTS.....	5
3.1 End-Fed Slotted Waveguide Antenna.....	5
3.2 Patch Array Antenna.....	9
4 ANALYSIS OF SLOTTED ARRAY RADIATION PATTERN	12
5 CONCLUSIONS	15
6 REFERENCES	16

FIGURES

	Page
Figure 1. Measurement setup.....	3
Figure 2. Slotted waveguide assembly with end of radome removed	5
Figure 3. Representative individual antenna patterns of the slotted array antenna	6
Figure 4. Density plot of slotted array radar antenna patterns across 8000-10800 MHz	6
Figure 5. Three-dimensional view of the slotted array antenna patterns of Figure 4	7
Figure 6. Emission spectra of the slotted array radar measured at three azimuths (main beam, +5°, and -5°), plus the peak (true) spectrum measured across all azimuths	8
Figure 7. Center-fed patch array antenna.....	9
Figure 8. Density plot of patch array radar antenna patterns across 8000-10800 MHz	10
Figure 9. Three-dimensional view of the patch array radar antenna patterns.....	10
Figure 10. Emission spectra of the patch array radar measured on one azimuth (main beam), plus the peak (true) spectrum measured across all azimuths.....	11
Figure 11. Modeled main-beam frequency dependence for the end-fed slotted array	13
Figure 12. Emission spectra in the primary and secondary antenna beams of the slotted array antenna	14

TABLES

Table 1. Slotted Waveguide Physical Parameters.....	12
---	----

ABBREVIATIONS/ACRONYMS

ITS	Institute for Telecommunication Sciences
ITU-R	International Telecommunication Union, Radiocommunication Sector
NTIA	National Telecommunications and Information Administration
RSEC	Radar Spectrum Engineering Criteria
RBW	resolution bandwidth
RSL	received signal level
OOB	out-of-band (emission type)
YIG	yttrium iron garnet (filter technology)

PHASED ARRAY ANTENNA PATTERN VARIATION WITH FREQUENCY AND IMPLICATIONS FOR RADAR SPECTRUM MEASUREMENTS

Frank H. Sanders¹ and Bradley J. Ramsey²

Measured antenna patterns of an end-fed slotted waveguide antenna and a phased-array patch antenna used in maritime radionavigation radars across the frequency range 8500-10800 MHz are presented along with a measurement technique that characterizes the antenna patterns as a function of frequency. The frequency-dependent variation in the measured pattern of the slotted waveguide is compared to the frequency dependence of an ideal pattern based on the slot geometry. The implications for radar emissions measurement techniques are discussed.

Key words: radar antenna pattern; radar emission measurement techniques; radar phased array antennas; Radar Spectrum Engineering Criteria (RSEC); squint angle

1 INTRODUCTION

Measurements of radiated emission spectra of radiolocation and radionavigation radar transmitters require that the peak emission level from the transmitters be obtained and recorded at each measured frequency in the spectrum. Methodologies for obtaining these maxima at each measured frequency when the radar beam is scanning through space are described in existing technical literature [1-4].

These references indicate that it is possible to obtain maximum amplitudes at frequencies across the emission spectrum if the radar antenna beam is not scanning. NTIA Report TR-05-420, "Measurement procedures for the Radar Spectrum Engineering Criteria," states, "measurements may be performed without the radar antenna being rotated, provided that the directions of both maximum fundamental emission and any unwanted emission are known [1, p. 79]." The ITU-R Recommendation M.1177 includes the same sentence [2, p. 16]. For radars that have not been characterized previously, this information is generally not known and the radar under test typically is boresighted in the direction of the measurement system. (Operationally, "boresighted" means that the radar's antenna is oriented so as to produce the maximum received signal level at a measurement system tuned to the fundamental frequency of the radar.) The advantage of making a measurement with the radar antenna fixed is that the peak received signal level (RSL) may be measured more quickly. Otherwise the system must be configured to select the peak reading from each full rotation or beam scan of the radar. While a stationary-antenna measurement technique can increase the speed of the measurement, it will only

¹ The author is with the Institute for Telecommunication Sciences, National Telecommunications and Information Administration, U.S. Department of Commerce, Boulder, CO.

² The author is with the RF Metrics Corporation, Westminster, CO.

provide relevant measurement data if the azimuth of the primary radiation lobe of the transmitting antenna relative to the mechanical structure of the antenna (the so-called squint angle) does not vary as a function of frequency.

Many phased-array radar antenna designs do not meet this requirement. The frequency dependence of the main antenna lobe is well understood [5, 6, 7], but despite the availability of antenna modeling techniques, these tools are not generally used by measurement organizations. Moreover the application of modeling techniques is dependent upon precise knowledge of physical antenna features that are usually obscured by a radome. This NTIA report describes the methodology for measuring frequency-dependent squint angle variations in such radar antenna patterns without the need for such knowledge. Two specific examples are presented in which the radiation patterns of 9300-9500 MHz maritime radionavigation antennas are measured across a frequency range of 8000-10800 MHz. The two radar antennas that are examined are an end-fed slotted array design and a phased-array patch design.

For the slotted array, the measurement data are compared with the computed squint angle frequency dependence for the slot geometry, and the results are demonstrated to be a close match. For the patch array, the design symmetry should produce no squint angle variation with frequency, but nevertheless some variation is observed in actual antenna pattern data. The implication of this work is that any radar antenna using a phased array design should be assumed to produce frequency-dependent variations in its radiation pattern even if such variations are predicted theoretically to be zero (or unless proven otherwise by antenna pattern measurement data).

Frequency-dependent variations will adversely affect radar emission spectrum measurement results if the radar antennas in question are boresighted on the measurement system, as demonstrated below in this report. Therefore, *radiated spectrum measurements of such radars should generally be performed while the radar antennas are actively rotating.*

2 APPROACH

Two maritime radionavigation radar transmitters operating in the 9300-9500 MHz band were operated at the Table Mountain field site north of Boulder, Colorado, for radiated emission spectrum measurements in accordance with the standard radiated measurement method [1-2]. The radars were positioned on a tower at a height of 3 m above the ground at a distance of 125 m from the measurement platform. Two separate measurement systems were used, each with its own antennas which were both mounted 3 m above the ground. A block diagram of this setup is shown in Figure 1.

System 1 was comprised of a 0.5-m diameter parabolic reflector antenna with a wideband 1-18 GHz feed antenna, a low-noise frequency-tracking preselector, and a spectrum analyzer to measure radiated antenna patterns between 8000-10800 MHz. The tracking preselector consisted of a variable-level step attenuator, a yttrium-iron-garnet (YIG) tunable bandpass filter, and a low-noise amplifier.

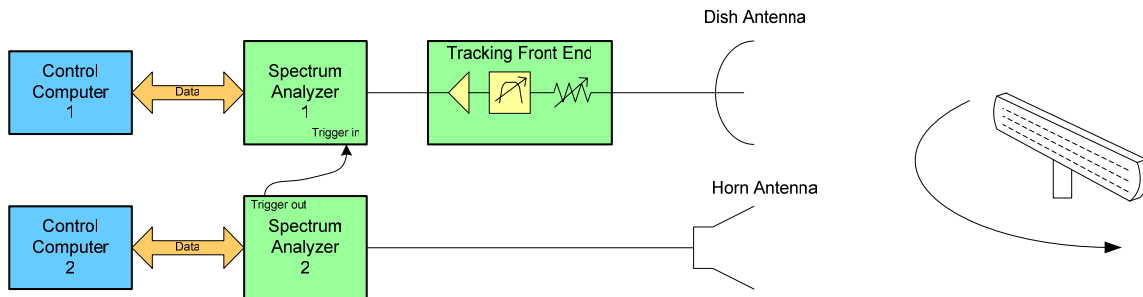


Figure 1. Measurement setup. Two spectrum measurement systems, System 1 (top), and System 2 (bottom) are used, with sweep triggering linked between them.

System 2 utilized a low-gain horn antenna and spectrum analyzer to capture antenna patterns at each radar's fundamental frequency. Spectrum analyzer 2 was configured to sweep when the received signal exceeded a level that was just below the peak of the emission pattern. The trigger produced by this event was routed to spectrum analyzer 1 in System 1. The result was two nearly simultaneous analyzer sweeps, one made by System 1 at each measurement frequency in the spectrum and the second made by System 2 at the radar's fundamental frequency.

The high gain and low gain antennas were co-located, with a separation distance of a few centimeters between them. By sharing a single trigger, the antenna patterns collected by Systems 1 and 2 were collected simultaneously, and the position of the primary antenna beam at the fundamental frequency in the trace data from System 2 could be directly compared with the azimuthal position of the emission patterns collected from System 1. Using this technique the variation of the patterns as a function of frequency could be determined. The coordinate system of the measurements was aligned azimuthally on the direction of the main beam of the radar at the radar fundamental frequency. (No elevation information was measured on the radar antenna pattern.)

The sweep time of both analyzers was set to an interval slightly longer than the rotation time of the radar—in this case, 3 seconds (as the radar rotation interval was approximately 2.5 sec). Both spectrum analyzers were set to single sweep mode.

Both systems operated under computer control. The spectrum analyzer in System 1 acquired measurements using a modified version of the standard stepped-frequency procedure for measuring radar emission spectra [1-2]. In this procedure, a radar emission spectrum is measured as follows. A spectrum analyzer is placed in a zero-hertz span mode, so that it measures received power as a function of time rather than frequency. Peak detection is selected, the analyzer IF bandwidth is selected at a value somewhat less than $(1/(\text{radar pulse width}))$, and the analyzer video bandwidth is adjusted to be slightly wider than the IF bandwidth. The analyzer sweep time is slightly longer than the radar antenna scan interval. A single sweep is taken on the analyzer at the selected frequency, revealing the fluctuating received signal from the radar as its beam is scanned through space. The highest-amplitude value is retrieved from that sweep and stored as the radar maximum emission amplitude at that frequency. Next, the spectrum analyzer tuned frequency is increased by an amount equal to the IF bandwidth (e.g., if the IF bandwidth is set to 8 MHz, the tuned frequency is stepped to a value 8 MHz higher than the previous tuned frequency). A single sweep is taken at the new frequency, the maximum value is recorded, and the process is continued until the entire radar emission spectrum has been measured in this manner. RF attenuation is added and removed as necessary throughout the measurement to keep the received power from the radar within the dynamic range of the measurement system. A tunable bandpass filter (usually a YIG technology device) is employed immediately after the RF attenuator to reject strong off-frequency energy, and a low-noise amplifier is used immediately after the filter to improve the sensitivity of the measurement system.

But in addition to obtaining maximum-power data with a peak detector at every frequency step in the spectrum, the controller computer was configured to record the entire antenna pattern at each measurement step. System 2 simultaneously recorded the antenna pattern at the fundamental frequency.

Thus, as the spectrum was built step by step in frequency, the antenna patterns at each measured frequency were likewise acquired and recorded, and their directions were all aligned relative to the main beam (fundamental frequency) azimuthal direction of the radar antenna by means of the main-beam-dependent triggering mechanism.

For these measurements, the radars were operated in their shortest pulse width modes (about 50 ns, equating to a 20-MHz bandwidth), allowing an 8-MHz resolution bandwidth (RBW) to be used for the measurement. The frequency increment between antenna pattern collections was accordingly set to 8 MHz. As a result, both spectrum power levels and antenna patterns were measured across the range of 8000-10800 MHz at 351 separate frequency steps.

3 RESULTS

3.1 End-Fed Slotted Waveguide Antenna

The first test unit was a marine radar using an end-fed slotted waveguide antenna. A photograph of the assembly inside the radome is shown in Figure 2. The radiating element is a waveguide with transverse slots cut at a spacing of 2.35 mm. A periodic fence in front of the waveguide provides additional directivity and sidelobe suppression.

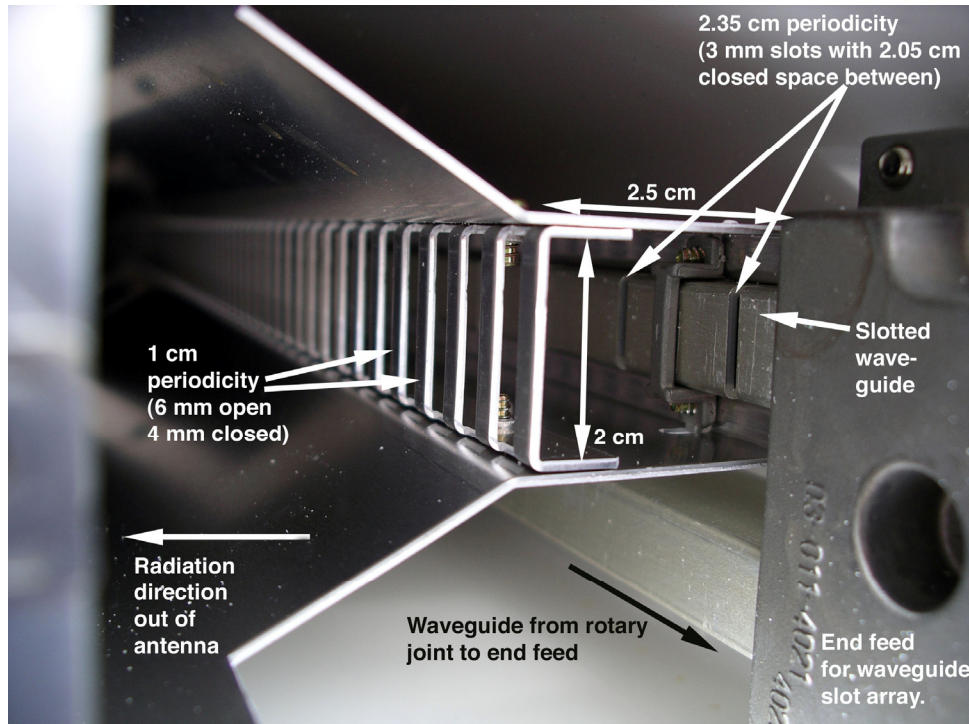


Figure 2. Slotted waveguide assembly with end of radome removed.

Examples of individual antenna patterns of the end-fed slotted array antenna are shown in Figure 3 at four frequencies. The top pattern was collected at the radar's fundamental frequency, 9408 MHz. The other antenna patterns are registered azimuthally relative to the direction of the main beam in the top pattern. A set of 351 such antenna patterns were recorded, including one at the fundamental frequency of the radar. These antenna patterns were automatically aligned azimuthally using software tools and combined into three-dimensional representations. Figures 4 and 5 were constructed by plotting all of the patterns in a single graph. Amplitudes in the patterns were color-coded to provide for easier interpretation of the resulting graphs. The pattern data are shown across azimuth angles of ± 20 degrees relative to the main beam direction at the fundamental. In presenting the data this way the frequency dependence of the main lobe in the pattern becomes immediately apparent. The main lobe in Figure 4 follows a curve that starts at +14 degrees azimuth at 8000 MHz and decreases to -8 degrees at 10500 MHz. The main lobe is at 0 degrees by definition at the radar's fundamental frequency of 9408 MHz.

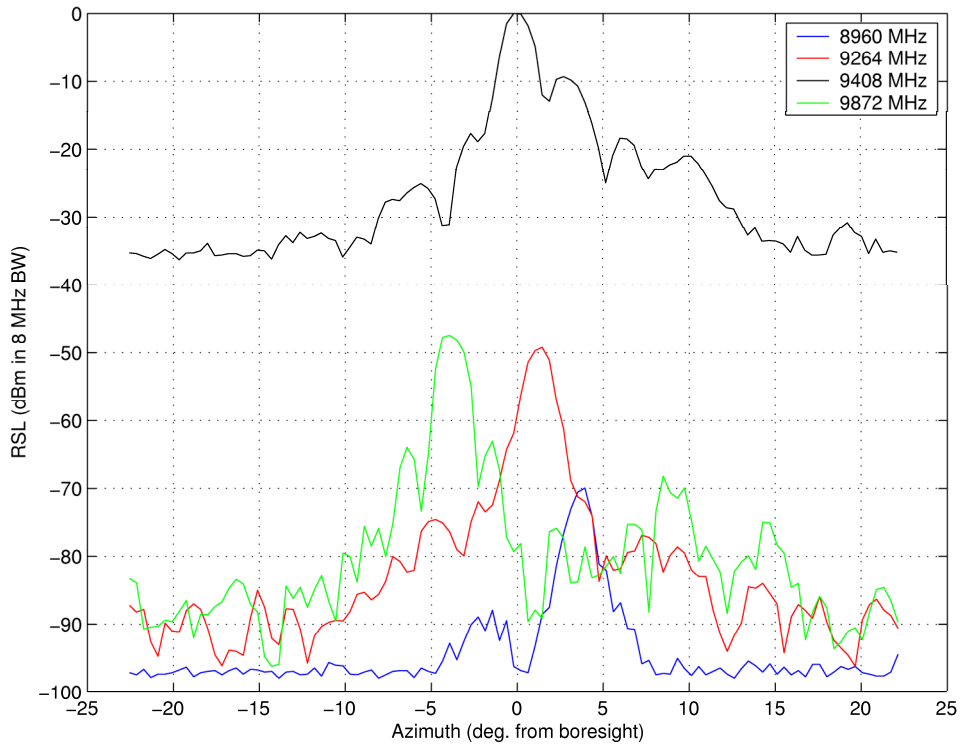


Figure 3. Representative individual antenna patterns of the slotted array antenna at four frequencies.

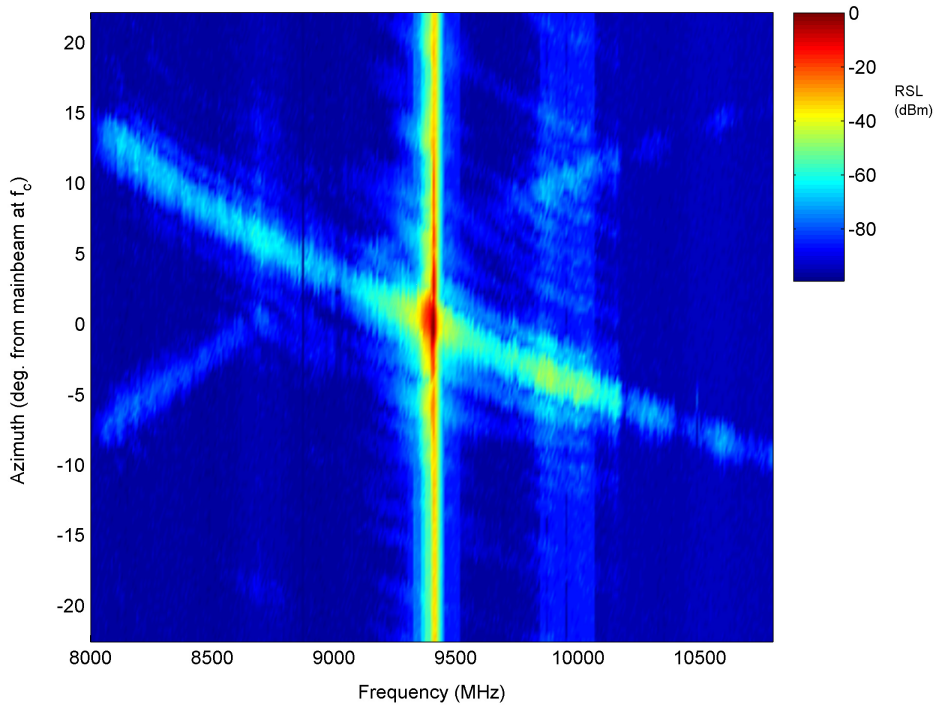


Figure 4. Density plot of slotted array radar antenna patterns across 8000-10800 MHz, between ± 20 degrees of the radar main beam direction.

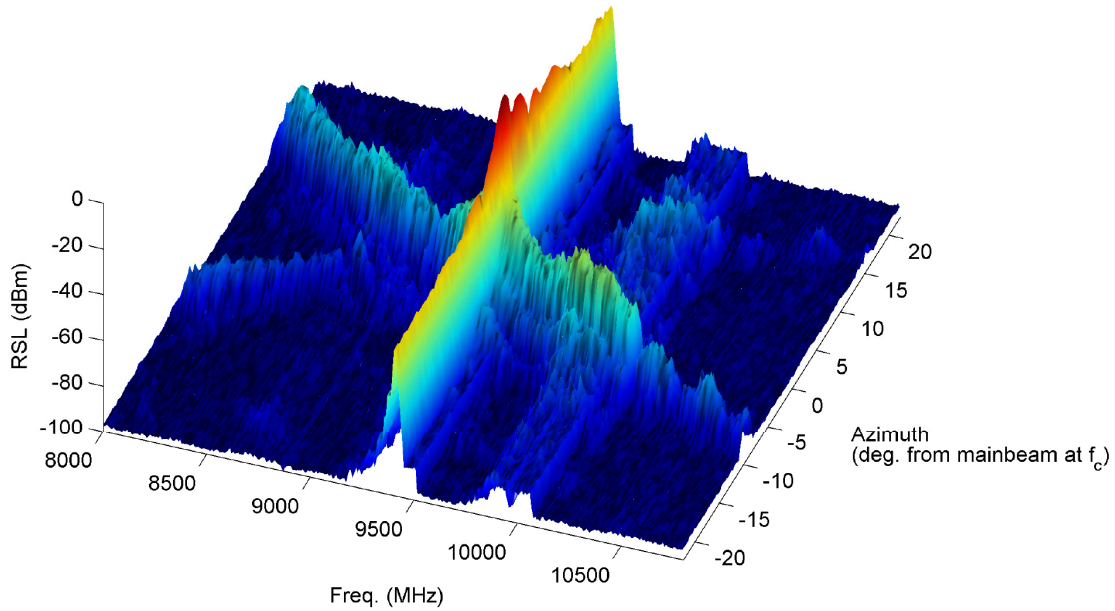


Figure 5. Three-dimensional view of the slotted array radar antenna patterns of Figure 4.

Using the dataset shown in Figures 4 and 5, measurement results at fixed azimuths from boresight can be synthesized. For example, if the data in Figure 4 are sliced using a plane positioned at 0 degrees azimuth, the resulting data will represent an emission measurement of the radar as though it were fixed in a boresighted configuration. By moving the plane to other azimuths, other configurations may be synthesized. Figure 6 shows the measurements at four separate azimuths according to the dataset. The peak of each measurement occurs at the same frequency, the fundamental of the radar. The emission spectrum characteristics at frequencies far from the fundamental show a significant variation with respect to the azimuth of the measurement system, with peak variations exceeding 15 dB. The curves indicate that out-of-band (OOB) and spurious emissions from this radar are directed off-axis with respect to the main lobe at the fundamental. Furthermore, the off-axis direction is frequency dependent. The peak emission spectrum, measured across all azimuths, is plotted as the black curve in Figure 6.

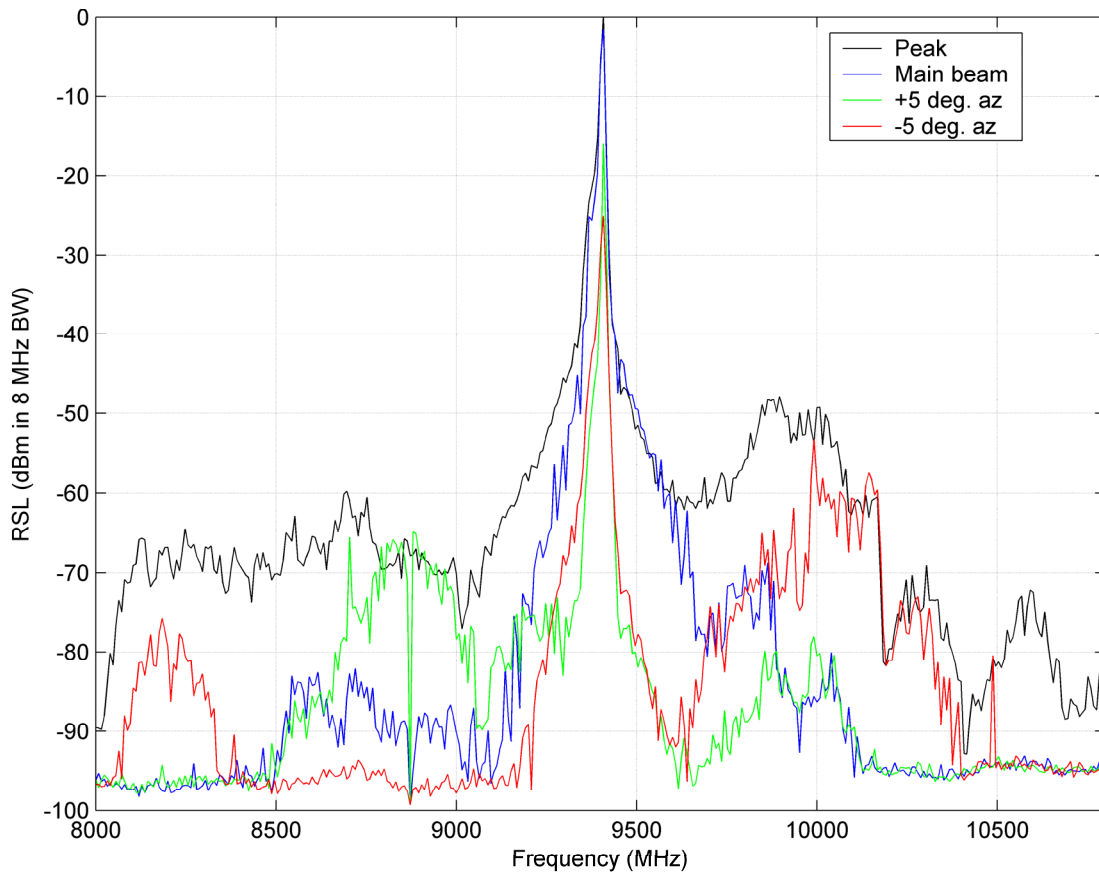


Figure 6. Emission spectra of the slotted array radar measured at three azimuths (main beam, +5°, and -5°), plus the peak (true) spectrum measured across all azimuths.

3.2 Patch Array Antenna

The second radar to be measured was a marine radar using a patch array antenna. A photograph of the antenna is shown in Figure 7. The antenna is fed from a waveguide that terminates at the top center of the patch array. The individual patches are arranged in columns of three, with each patch fed from a microstrip line. Columns are connected to a microstrip line that follows the top edge of the array so that each column receives a fixed phase delay from the center point.

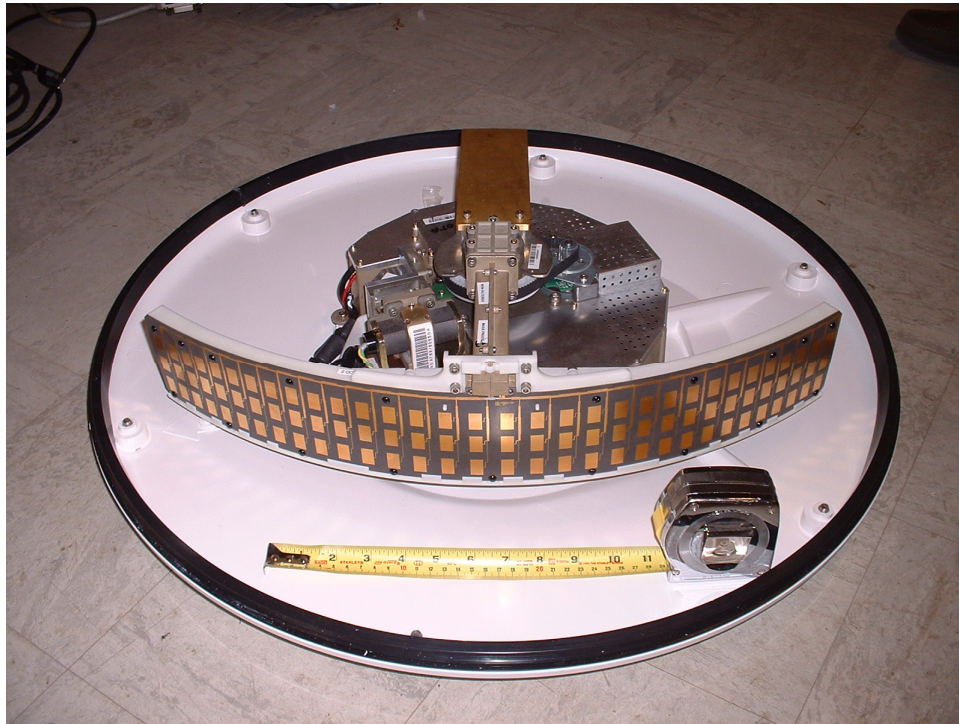


Figure 7. Center-fed patch array antenna.

Figures 8 and 9 show pattern data for the patch array radar antenna. As in the slotted waveguide array, the patterns display a frequency dependency with respect to the maximum emission azimuth in the OOB region. Figure 10 shows the difference in measured spectra between measuring the radar while rotated (the peak curve) and measuring at the boresight azimuth only (the main beam curve). While the differences are less than for the slotted waveguide case, they do exceed 10 dB in portions of the spectrum. For existing and future standards this discrepancy could mean the difference between meeting the emission specification or failing.

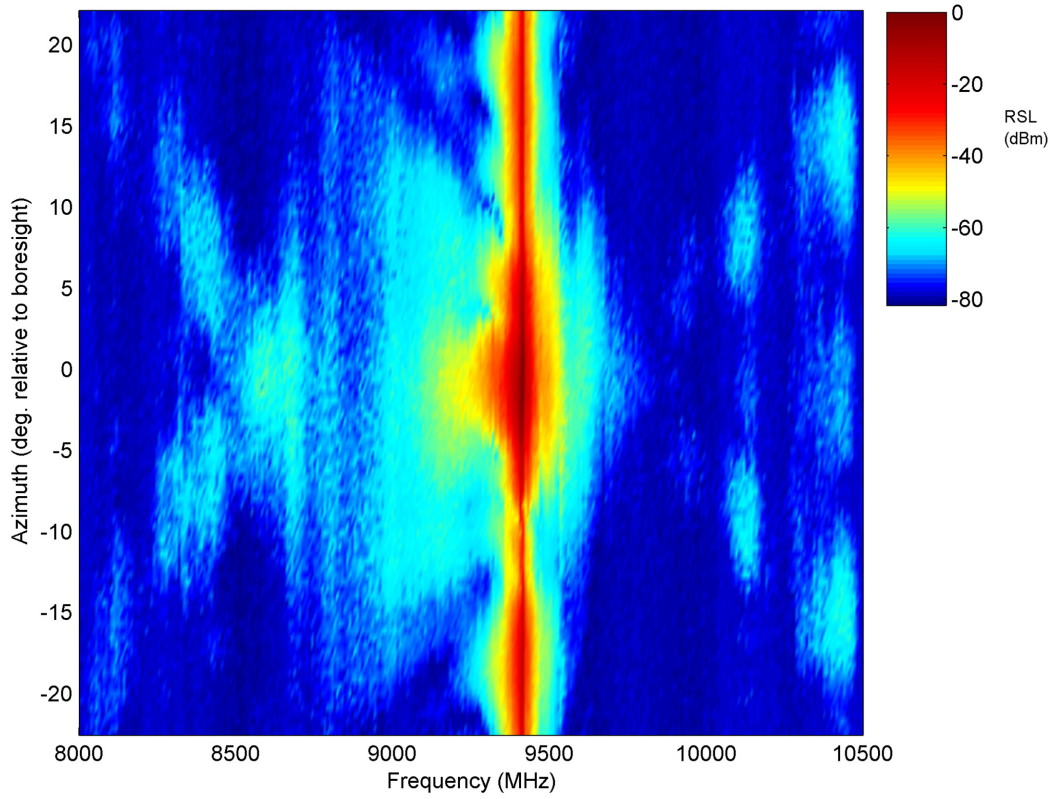


Figure 8. Density plot of patch array radar antenna patterns across 8000-10800 MHz, between ± 20 degrees of the radar main beam direction.

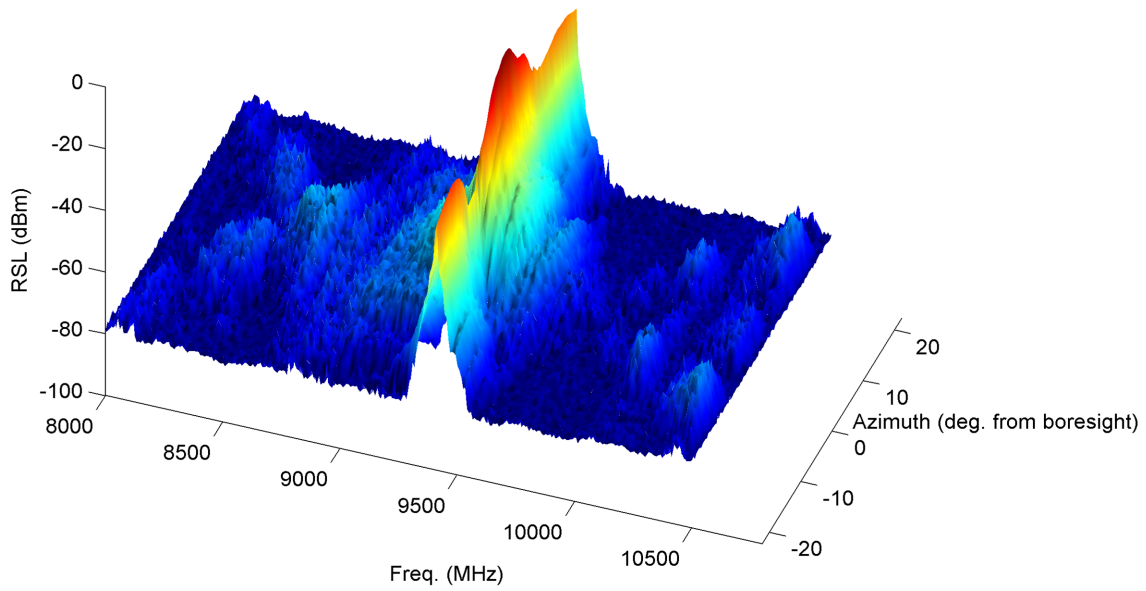


Figure 9. Three-dimensional view of the patch array radar antenna patterns of Figure 8.

The patch array is symmetrically fed from the center. Theoretically, it should not exhibit an asymmetric frequency-dependent pattern for the main beam such as that observed for the slotted array. But the data in Figures 8 and 9 show clearly that, while the frequency-dependent radiation patterns of the patch array are approximately symmetrical, there are significant off-boresight emissions.

The practical upshot of this effect, however, is that the azimuth of the strongest radiation from the patch array at any given frequency cannot be expected to be in the same direction as the main beam at the fundamental frequency of the antenna.

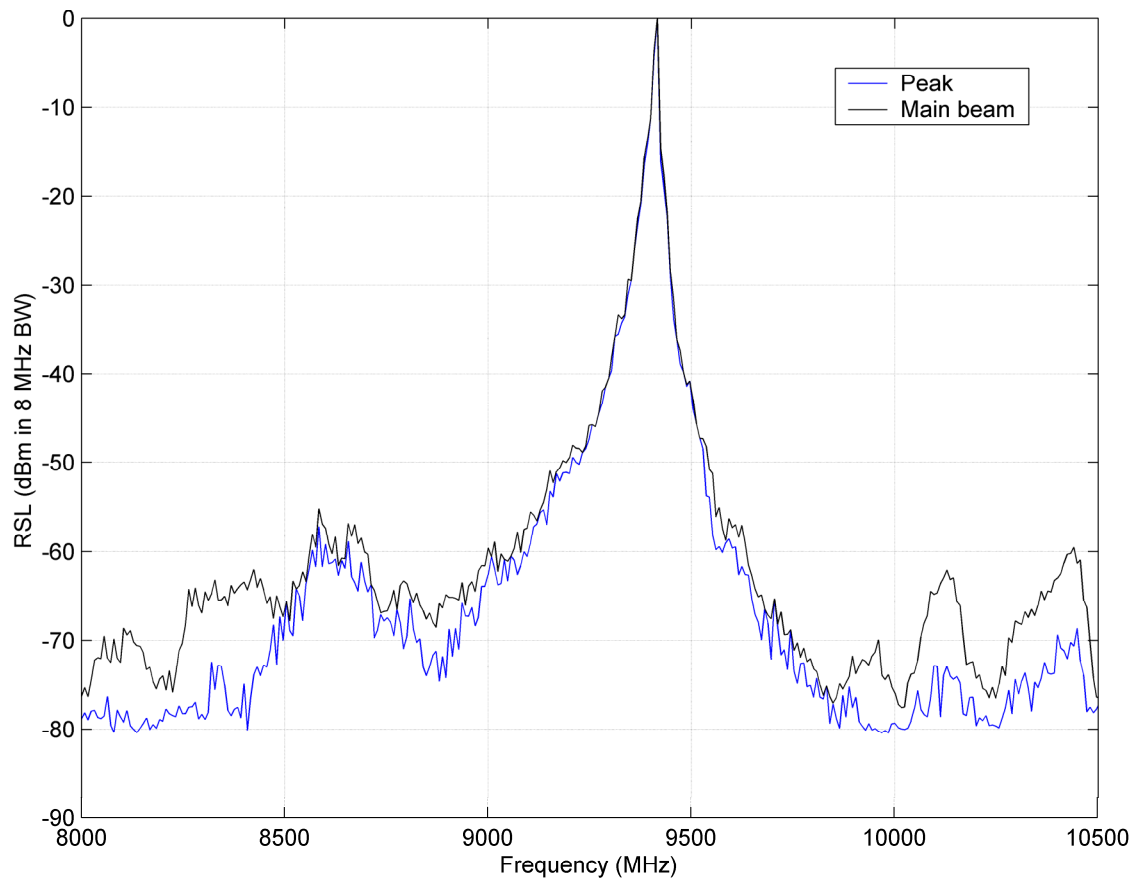


Figure 10. Emission spectra of the patch array radar measured on one azimuth (main beam), plus the peak (true) spectrum measured across all azimuths.

4 ANALYSIS OF SLOTTED ARRAY RADIATION PATTERN

Based on the geometry of the slotted array the squint angle can be computed. The geometry of the end-fed slotted array is given in Table 1.

Table 1. Slotted Waveguide Physical Parameters

Dielectric Material	Air
Waveguide width, x_0	0.8 cm
Waveguide height y_0	0.4 cm
Slot spacing s	2.35 cm
Mode Number k	0

The wavelength inside the guide for mode $TE_{m,n}$ is given by [6, p. 304]:

$$\lambda_{g,m,n} = \frac{\lambda}{\left[\varepsilon - (m\lambda/2x_0)^2 - (n\lambda/2y_0)^2 \right]^{1/2}} \quad (1)$$

where ε is the dielectric constant for the medium inside the guide. For a TE_{10} wave in a waveguide with dimensions given in Table 1:

$$\lambda_g = 5.10 \text{ cm at } 9408 \text{ MHz.}$$

The direction of the main lobe for a slotted array is given by [7]:

$$\phi = \cos^{-1} \left[\frac{\lambda}{\lambda_g} + \frac{k}{s/\lambda} \right] \quad k = 0, \pm \frac{1}{2}, \pm 1, \dots \quad (2)$$

where s is the slot spacing and m is the mode number from Table 1. Figure 11 is a plot of the same pattern data shown in Figure 4 with a curve computed from (2) added using $k = 0$. The computed squint angle of the main lobe agrees well with the measured squint angle. A second prominent lobe has inverted frequency dependence, indicative of a reflected wave in the waveguide. This second lobe should be absent, based on the assumption that the termination end of the waveguide (opposite the feed end) is a perfect absorber of the stray energy that has traversed the length of the antenna. The fact that this weaker, mirror-image secondary beam *is* observed implies that the termination end of the antenna waveguide is not acting as a very effective absorber. As the reflected energy from the poor termination encounters the slotted array in a reversed direction relative to the desired radiation energy, the secondary beam of the antenna is reversed in orientation relative to the main beam. It is not known whether the waveguide termination at the end of the measured antenna was defective or damaged, or whether the inefficient absorption at that point resulted from some sort of economy related to the antenna manufacturing process. Together, the directions of these two beams form a sort of X in the antenna

pattern space of Figure 11. They converge somewhat away from the main beam of the radar at its fundamental frequency.

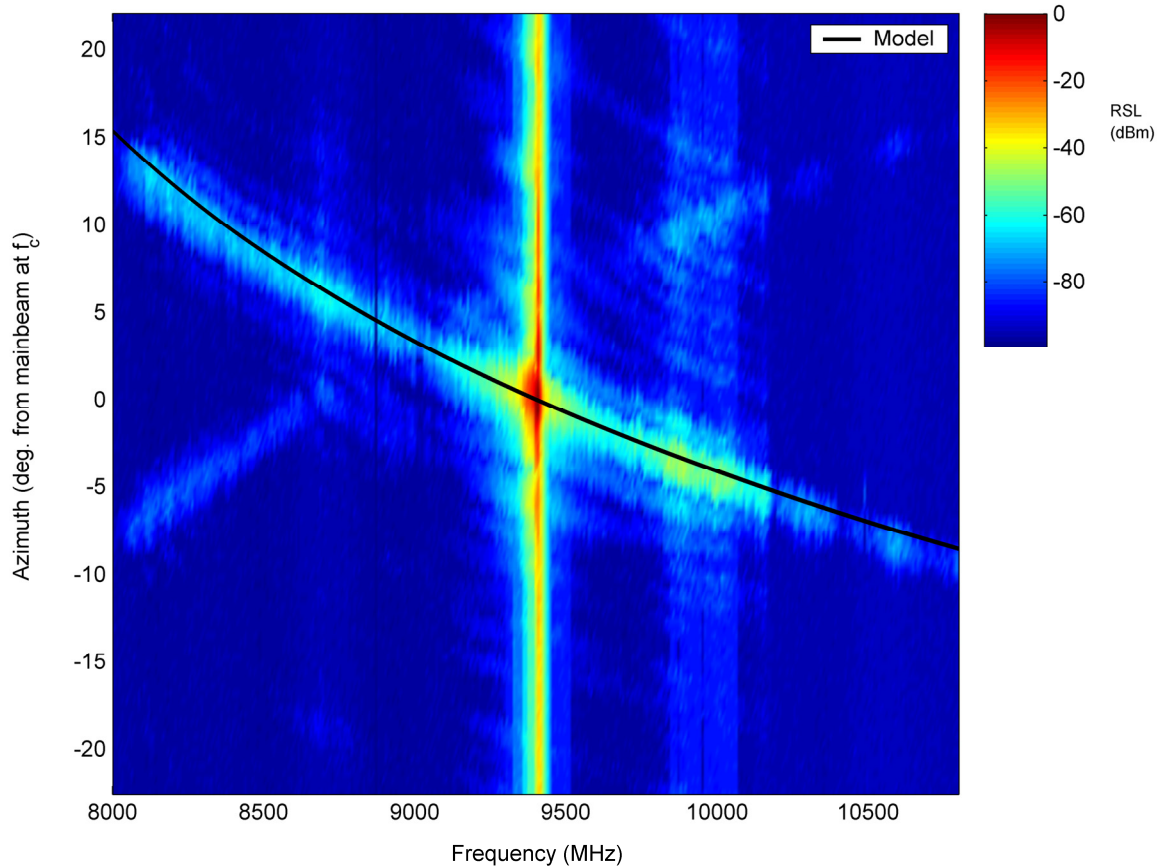


Figure 11. Modeled main-beam frequency dependence (black line) for the end-fed slotted array using the actual waveguide dimensions, plotted on top of measurement data.

In addition to the secondary beam, lower-amplitude beams form as well, appearing as smaller structures parallel to the primary beam. They also change direction at a rate of about -8 degrees per gigahertz across the range of the measurement. They are manifested as conventional side lobes in the antenna pattern at the fundamental frequency.

The radar spectrum as measured along each of the two beams is shown in Figure 12. It is apparent from this figure that emissions from the secondary beam do not contribute to the peak measurement, since the secondary-beam spectrum never exceeds the primary-beam spectrum. The primary beam is a single, distinct beam that consistently has the highest amplitude.

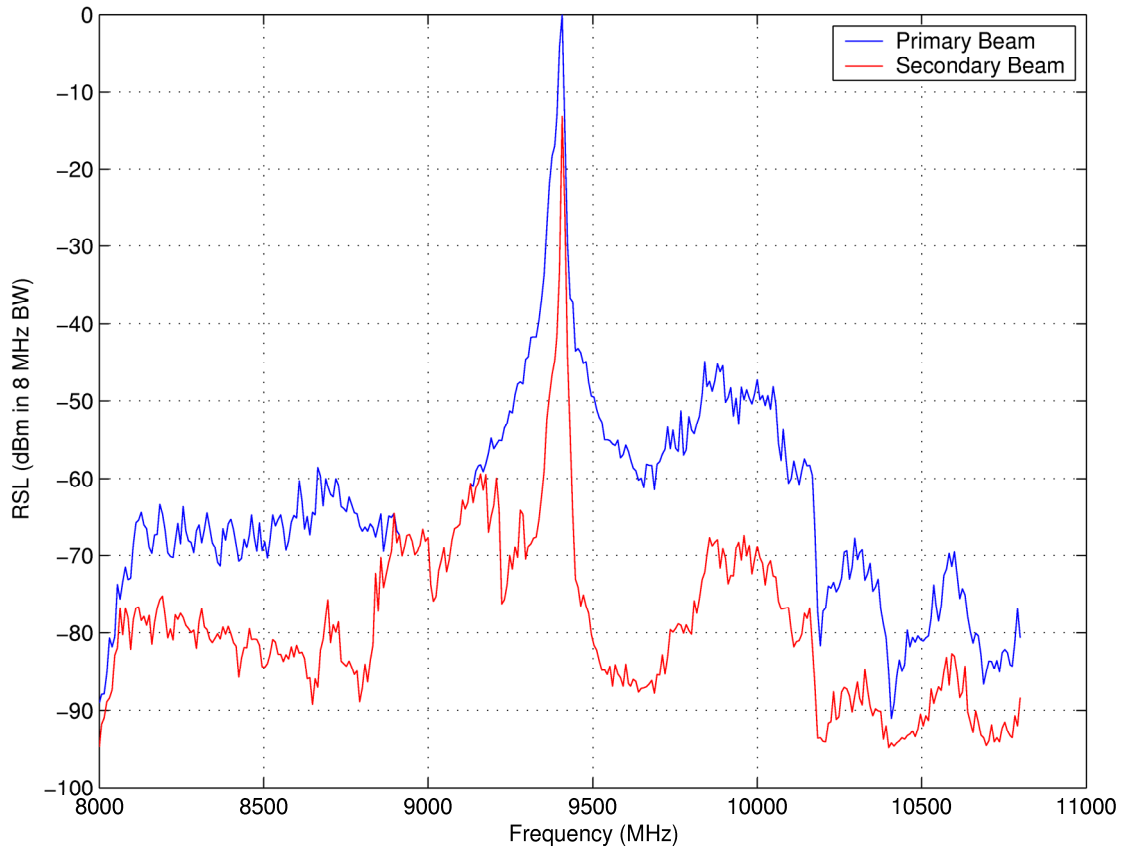


Figure 12. Emission spectra in the primary and secondary antenna beams of the slotted array antenna.

5 CONCLUSIONS

Radar antennas that form a beam using the phase differences between multiple discrete radiating apertures, such as slotted arrays and patch arrays, typically will not form the main beam of radiation in a fixed direction in space relative to the antenna structure as the frequency of the radiation changes through the emission spectrum. This frequency-dependent squint-angle effect is predicted theoretically as a first-order effect for non-symmetrically fed arrays (such as end-fed slotted arrays), and may still occur even for symmetrically fed arrays (such as center-fed patch arrays) as an apparent second-order effect.

A measurement technique has been developed to observe and measure this effect throughout the measurement of wideband emission spectra of radar transmitters. Example measurements using the technique have shown both the effects described above for end-fed slotted array and patch array antennas.

Due to these effects, radiated radar spectrum emission measurements should be performed while radar beams are rotated (or otherwise scanned) through space in a normal operational mode, using standard stepped-frequency techniques [1-2].

The measurement technique described in this report may be generally applied to the characterization of radar antenna patterns across wide frequency ranges. The data may be useful and necessary in some electromagnetic compatibility analyses. Such data may be acquired simultaneously with the acquisition of radiated radar emission spectra; no time is lost in this type of measurement relative to a spectrum-only measurement. The only additional cost is the requirement for the use of a second spectrum analyzer and antenna during the measurement and the required analysis software.

6 REFERENCES

- [1] F.H. Sanders, R.L. Hinkle, and B.J. Ramsey, "Measurement procedures for the Radar Spectrum Engineering Criteria," NTIA Report TR-05-420, Mar. 2005.
- [2] ITU-R Recommendation M.1177, "Techniques for measurement of unwanted emissions of radar systems," International Telecommunication Union, Radiocommunication Sector, 2003.
- [3] F.H. Sanders, "Bandwidth dependence of emission spectra of selected pulsed-CW radars," NTIA Technical Memorandum TM-05-431, Aug. 2005.
- [4] F.H. Sanders and B.J. Ramsey, "Comparison of radar spectra on varying azimuths relative to the base of the antenna rotary joint," NTIA Technical Memorandum TM-05-430, Aug. 2005.
- [5] R.J. Mailloux, *Phased Array Antenna Handbook*, Boston: Artech House, 1994, pp. 292-296.
- [6] T. Itoh, "Waveguides and resonators," *Reference Data for Engineers*, M. Van Valkenburg, ed., Boston: Newnes, 1998, p. 30-4.
- [7] J.D. Krauss, *Antennas, Second Edition*, New York: McGraw-Hill, 1988.

BIBLIOGRAPHIC DATA SHEET

1. PUBLICATION NO. TR-06-436		2. Government Accession No.	3. Recipient's Accession No.
4. TITLE AND SUBTITLE Phased Array Antenna Pattern Variation with Frequency and Implications for Radar Spectrum Measurements		5. Publication Date December 2005	
		6. Performing Organization Code NTIA/ITS	
7. AUTHOR(S) Frank H. Sanders and Bradley J. Ramsey		9. Project/Task/Work Unit No. 511 3105011-300	
8. PERFORMING ORGANIZATION NAME AND ADDRESS NTIA/ITS.T U.S. Department of Commerce 325 Broadway Boulder, CO 80305		10. Contract/Grant No.	
		11. Sponsoring Organization Name and Address	
11. Sponsoring Organization Name and Address		12. Type of Report and Period Covered	
14. SUPPLEMENTARY NOTES			
15. ABSTRACT (A 200-word or less factual summary of most significant information. If document includes a significant bibliography or literature survey, mention it here.) Measured antenna patterns of an end-fed slotted waveguide antenna and a phased-array patch antenna used in maritime radionavigation radars across the frequency range 8500-10800 MHz are presented along with a measurement technique that characterizes the antenna patterns as a function of frequency. The frequency-dependent variation in the measured pattern of the slotted waveguide is compared to the frequency dependence of an ideal pattern based on the slot geometry. The implications for radar emissions measurement techniques are discussed.			
16. Key Words (Alphabetical order, separated by semicolons) radar antenna pattern; radar emission measurement techniques; radar phased array antennas; Radar Spectrum Engineering Criteria (RSEC); squint angle			
17. AVAILABILITY STATEMENT UNLIMITED.		18. Security Class. (This report)	20. Number of pages 101
		19. Security Class. (This page)	21. Price:

NTIA FORMAL PUBLICATION SERIES

NTIA MONOGRAPH (MG)

A scholarly, professionally oriented publication dealing with state-of-the-art research or an authoritative treatment of a broad area. Expected to have long-lasting value.

NTIA SPECIAL PUBLICATION (SP)

Conference proceedings, bibliographies, selected speeches, course and instructional materials, directories, and major studies mandated by Congress.

NTIA REPORT (TR)

Important contributions to existing knowledge of less breadth than a monograph, such as results of completed projects and major activities. Subsets of this series include:

NTIA RESTRICTED REPORT (RR)

Contributions that are limited in distribution because of national security classification or Departmental constraints.

NTIA CONTRACTOR REPORT (CR)

Information generated under an NTIA contract or grant, written by the contractor, and considered an important contribution to existing knowledge.

JOINT NTIA/OTHER-AGENCY REPORT (JR)

This report receives both local NTIA and other agency review. Both agencies' logos and report series numbering appear on the cover.

NTIA SOFTWARE & DATA PRODUCTS (SD)

Software such as programs, test data, and sound/video files. This series can be used to transfer technology to U.S. industry.

NTIA HANDBOOK (HB)

Information pertaining to technical procedures, reference and data guides, and formal user's manuals that are expected to be pertinent for a long time.

NTIA TECHNICAL MEMORANDUM (TM)

Technical information typically of less breadth than an NTIA Report. The series includes data, preliminary project results, and information for a specific, limited audience.

For information about NTIA publications, contact the NTIA/ITS Technical Publications Office at 325 Broadway, Boulder, CO, 80305 Tel. (303) 497-3572 or e-mail info@its.blrdoc.gov.

This report is for sale by the National Technical Information Service, 5285 Port Royal Road, Springfield, VA 22161, Tel. (800) 553-6847.

